Short Communications

Ultrastructural and seasonal aspects of the kidney lymphatic system of hibernating animals

G. Azzali

Institute of Anatomy, Medical School, University of Parma, Via Gramsci 14, I-43100 Parma (Italy)
Received 22 July 1987; accepted 28 January 1988

Summary. The kidney lymphatic system of bat, dormouse and marmot consists of intraparenchymal (interlobar, arcuate, interlobular) and extraparenchymal (capsular) vessels sharing common ultrastructural aspects. We did not observe medullary lymphatics. The qualitative and quantitative seasonal changes in the ultrastructure of the lymphatic endothelium represent not only a species-linked feature but also (and mainly) an evident seasonal fluctuation in lymph formation. Furthermore, these ultrastructural changes emphasize the important role played by the different mechanisms involved in the translymphatic movement of proteins and interstitial fluid with particular regard to the 'vesicular route' and intraendothelial channels.
Key words. Lymphatic vessels; kidney; ultrastructure; hibernation; seasonal changes.

Current opinions about the distribution and density of kidney lymphatics are quite discordant [1-4]. The role played by the lymphatic system in renal function and the extent to which renal filtration and tubular reabsorption contribute to lymph formation are also a subject of debate [5, 6]. In fact, as is exhaustively discussed by O'Morchoe [7] in his monograph, where as the existence of lymphatics in the cortex is unanimously accepted, different authors disagree about the drainage of interlobular vessels into capsular vessels [5-8] and about the connections between the lymphatic vessels and the afferent arteriole and other nephron components [2, 9-12]. A few years ago a debate developed about the existence of lymphatic vessels in the renal medulla. These controversies were difficult to resolve owing to poorly detailed descriptions [1, 11, 13], and also because the techniques of injection employed were considered unreliable by most authors [14]. Furthermore, physiological studies [15] seem to emphasize that the renal medulla contributes to the renal hilum lymph formation by movement of fluid from the medullary interstitium into arcuate and interlobar lymphatics. With regard to this, O'Morchoe [14] asserts that medullary lymphatics, whenever they exist at all, are so scarce and so far from each other that their morphological and functional role should be considered to be of no account.

The present study was carried out to describe the vascular lymphatic system of the kidney in some hibernating mammalians (bat, dormouse, marmot) in order to assess the topographical distribution of vessels, their relationships and ultrastructural aspects (related to biological and metabolic seasonal conditions) and the possible mechanisms involved in lymph formation.

Materials and methods. 70 bats (*Rinolophus ferrum equinum, Eptesicus serotinus, Pipistrellus kuhli kuhli*), 8 dormice (*Myoxus glis*) and 6 marmots (*Marmota marmota*) were captured and killed in different seasons. The animals were previously anesthetized with ethyl ether or sodium pentobarbital (Nembutal). Lymphatics were demonstrated using Ottaviani and Giacomelli's technique [16] by direct injection of standard dyes (Prussian blue, Neoprene latex) or by retrograde injection via renal hilar nodes.

For electron microscopy, small blocks of renal parenchyma (2–3 mm) were fixed (glutaraldehyde 3.5%, osmic acid 1% in cacodylate buffer at pH 7.3), dehydrated in acetone and embedded in Durcupan. Thick sections (1 μm), stained with toluidine blue, were utilized to identify the vascular bundle containing the lymphatic vessel and to center it during the cutting of the specimen. Ultrathin sections (750 Å thick), stained with lead citrate according to Reynolds [17], were examined with a Philips 300 electron microscope. We performed a morphometric analysis on 54 lymphatic vessels subdivided into two groups of 27 vessels each (10 from bats, 7 from dormice, 10 from marmots) obtained from animals killed during hibernation and summer, respectively. In particular we measured the numerical density, volume density and mean diameter of the different categories of uncoated vesicles lying in the non-nuclear cytoplasmic area of the endothelial cells of the two groups by means of a Zeiss Videoplan image analyser which was programmed to provide this information. We classified as 'luminal' or 'abluminal' the vesicles which either touched or were continuous with the plasma membrane, whereas 'cytoplasmic' vesicles appeared to be totally surrounded by endothelial cyto-

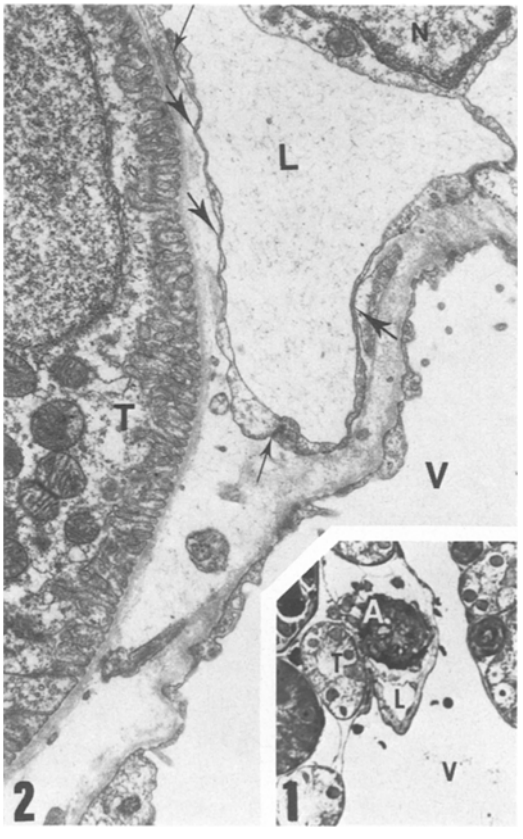

Figures 1 and 2. *Rinolophus f.e.* killed during hibernating period. Kidney-cortex. Fig. 1. Lymphatic vessel (L) lying in the connective tissue interposed between interlobular artery (A) and vein (V). A small segment of the lymphatic endothelial wall lies adjacent to a distal convoluted tubule (T). ×350. Fig. 2. Interlobular lymphatic (L) characterized by a linear endothelial wall and cytoplasmic expansions showing extremely slender segments (thick arrow) alternating with thicker segments. Luminal and abluminal uncoated vesicles are scarce. Thin arrow = overlapping and end to end intercellular junctions. V = interlobular vein. T = distal convoluted tubule. N = endothelial cell nucleus. ×10,800.

plasm[18]. A statistical analysis was performed with a non-parametric Wilcoxon rank sum test. The values are expressed as mean ± SD. A three-dimensional reconstruction (from ultrathin serial sections) of several segments (ranging from 160 to 300 nm in length) of the endothelial wall was carried out in 6 lymphatics (3 in the hibernating period and 3 in summertime) by means of Born's wax-disk technique recently revised by Werner[19].

Results and discussion. The injection of standard dyes into hilar nodes showed lymphatic vessels lying in the renal cortex and accompanying interlobar, arcuate and interlobular blood vessels as already described in man and other mammals[2, 9, 11, 13, 20, 21]. We also detected lymphatic vessels in the capsule and in the connective tissue interposed between the calyx wall and the renal parenchyma. Dormouse and marmot interlobular lymphatics of the cortex corticis drain directly into the capsular lymphatics. This morphological feature was not observed in bats. Similar results were obtained in sheep[22] and calf[2]. Furthermore, capsular lymphatics continue as precollecting vessels. Therefore lymph drains into hilar nodes by means of prenodal collecting lymphatics. The above reports, though obtained by a technique that is not fully reliable[14], were confirmed by light microscopic studies which revealed in more detail the disposition of the lymphatic vessel in the vascular bundle (fig. 1) and its relations with blood vessel[3, 4, 8, 9], renal corpuscles, proximal and distal convoluted tubules[2, 5, 9–11]. We did not detect lymphatics in renal medulla, in contrast with Rhodin[1], Cockett et al.[23] and Cuttino et al.[13].

Electron microscopy indicated that intra- and extraparenchymal vessels share common ultrastructural aspects. The endothelial wall is formed by a single layer of flat cells lacking basal lamina and fenestrations (fig. 2). Each endothelial cell, rectangular in shape, has a nuclear area and a large laminar, cytoplasmic expansion whose peripheral edges are joined to neighboring cells by means of end to end, overlapping and interdigitating junctions. In these cells we observed significant ultrastructural seasonal changes.

During hibernation the endothelial wall shows a linear profile (figs 2, 4). Extremely thin segments of the cytoplasmic expansion (40 nm in bat, 60 nm in dormouse and 80 nm in marmot) lacking vesicles alternate with thicker segments (110–180 nm) whose cytoplasma contains free ribosomes and uncoated vesicles. The intercellular junctions are of the overlapping and interdigitating type. *During summer* the endothelial wall (fig. 3) looks wavy and winding. The cytoplasmic expansion thickness is on the average 230 nm in bat, 290 nm in dormouse and 350 nm in marmot. The matrix of the cytoplasmic expansion is particularly rich in ribosomes, rough endoplasmic reticulum, luminal and abluminal uncoated vesicles (fig. 3 and inset a). The vesicles lying free within the cytoplasm ('cytoplasmic vesicles') are often arranged in a chain-like way across the endothelial surfaces.

Figure 3. *Rinolophus f.e.* killed during summertime. Kidney–cortex. Interlobular lymphatic (L) interposed between artery (A) and two convoluted tubules (T). The endothelial wall is formed by more cells whose laminar cytoplasmic expansions show a wavy profile and an abundant cytoplasm rich in ribosomes, RER tubules, luminal and abluminal vesicles (inset a, arrows). N = endothelial cell nucleus. ×10,800; ×27,000.

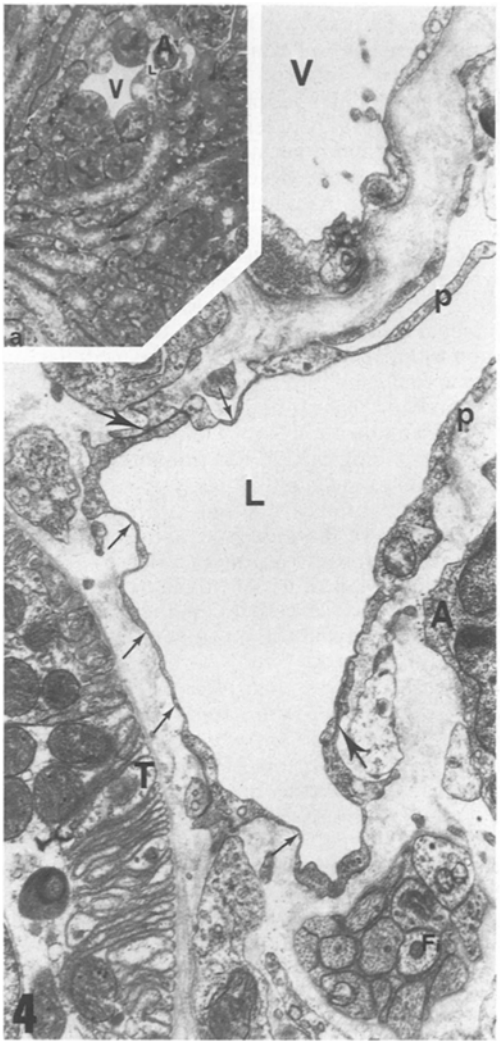

Figure 4. Marmot killed during hibernating period. Kidney–cortex. Acurate lymphatic (L) interposed between artery (A), vein (V) and a distal convoluted tubule (T) see also inset a. Endothelial wall formed by cytoplasmic expansions (p) showing several extremely slender segments (thin arrows). At this level luminal and abluminal membranes enclose a scanty cytoplasmic matrix mostly amorphous. Fi = amyelinic nervous fiber close to the lymphatic endothelial wall. Thick arrows = intercellular junctions. ×104; ×17,700.

Table 1. Bat (mean values ± SD)

Vesicles	Hibernation	Summer	
	Vv	Vv	p
Luminal	2.14 ± 0.8	7.07 ± 1.7	< 0.01
Abluminal	0.64 ± 0.23	3.33 ± 1.42	< 0.01
Cytoplasmic	21.05 ± 8.2	12.42 ± 5.78	< 0.05
	Nv	Nv	p
Luminal	12.02 ± 5.81	28.51 ± 6.5	< 0.01
Abluminal	3.6 ± 1.2	13.6 ± 4.5	< 0.01
Cytoplasmic	128.02 ± 20.2	46.42 ± 10.6	< 0.05
	$\bar{D}$	$\bar{D}$	$\bar{p}$
Luminal	70.1 ± 3.3	78.61 ± 3.4	n.s.
Abluminal	70.32 ± 2.8	78.02 ± 5.3	n.s.
Cytoplasmic	68.02 ± 1.2	80.4 ± 3.9	n.s.

Abbreviations: Vv = volume density ($\mu m^3/\mu m^3$); Vv, $\times 10^{-3}$; Nv = numerical density (number/μm^3); $\bar{D}$ = mean diameter (nm); n.s. = not significant.

Table 2. Dormouse (mean values ± SD)

Vesicles	Hibernation	Summer	
	Vv	Vv	p
Luminal	1.64 ± 0.76	3.4 ± 1.0	< 0.05
Abluminal	0.82 ± 0.24	1.79 ± 0.8	< 0.05
Cytoplasmic	17.40 ± 5.6	7.49 ± 2.0	< 0.01
	Nv	Nv	p
Luminal	9.2 ± 5.32	19.02 ± 6.4	< 0.01
Abluminal	4.61 ± 1.53	10.7 ± 3.34	< 0.01
Cytoplasmic	97.21 ± 10.8	28.21 ± 7.02	< 0.01
	$\bar{D}$	$\bar{D}$	$\bar{P}$
Luminal	70.02 ± 3.5	70.1 ± 4.12	n.s.
Abluminal	70.31 ± 3.71	70.06 ± 4.36	n.s.
Cytoplasmic	70.6 ± 3.38	79.91 ± 4.9	n.s

Abbreviations: Vv = volume density ($\mu m^3/\mu m^3$); Vv, $\times 10^{-3}$; Nv = numerical density (number/μm^3); $\bar{D}$ = mean diameter (nm); n.s. = not significant.

Table 3. Marmot (mean values ± SD)

Vesicles	Hibernation	Summer	
	Vv	Vv	p
Luminal	2.16 ± 1.26	5.36 ± 2.06	< 0.05
Abluminal	0.93 ± 0.3	3.49 ± 1.41	< 0.01
Cytoplasmic	27.21 ± 6.3	11.48 ± 5.46	< 0.05
	Nv	Nv	p
Luminal	10.2 ± 5.60	21.51 ± 8.22	< 0.01
Abluminal	5.21 ± 2.37	14.1 ± 5.26	< 0.01
Cytoplasmic	106.4 ± 16.02	30.12 ± 4.27	< 0.01
	$\bar{D}$	$\bar{D}$	$\bar{p}$
Luminal	74.2 ± 3.20	78.2 ± 3.9	n.s.
Abluminal	70.1 ± 2.81	78.06 ± 3.31	n.s.
Cytoplasmic	78.8 ± 0.8	90.01 ± 4.0	n.s.

Abbreviations: Vv = volume density ($\mu m^3/\mu m^3$); Vv, $\times 10^{-3}$; Nv = numerical density (number/μm^3); $\bar{D}$ = mean diameter (nm); n.s. = not significant.

The numerical density, volume density and mean diameter for the different categories of uncoated vesicles are shown in tables 1–3. The quantitative analysis of the uncoated vesicles shows that both the numerical density and the volume density of the luminal and abluminal vesicles are significantly increased in summer. This increase is evident in all the species investigated. In contrast, cytoplasmic vesicles increase significantly in number during hibernation in all the species: this observation, together with the scarcity of luminal and abluminal uncoated vesicles, provides further evidence for a reduced translymphatic movement of interstitial fluid and particles in this period of the year.

The mean diameter of the different categories of uncoated vesicles is almost constant both during hibernation and in summer. These data, besides confirming the important role of the 'vesicular route', bring into evidence a summer increase of the transendothelial transport activity, in agreement with previous reports on dogs under experimental conditions of increased lymph formation [24, 25]. In the same way the endothelial wall shows a strong numerical increase of luminal and abluminal cytoplasmic projections very similar to those observed in other mammals [5, 21]. These projections, in three-dimensional models obtained by serial ultrathin sections, appear as channel-like structures 4–7 µm in length similar to those that we described in other organs [26–28]. These channels must be considered as dynamic structures that the endothelium is able to form under particular physiological conditions (in response to unknown stimulating factors) which could allow a fast, non-selective passage of interstitial substances into the lymphatic lumen [29].

The ultrastructural changes of the lymphatic endothelium are only in part species-linked, but are clearly related to the peculiar biological and metabolic condition of the hibernating animals [30]. We think that these morphological changes indicate a clear seasonal fluctuation of the lymph flow. Furthermore, the significant summer increase of the luminal and abluminal uncoated vesicles indicates an important involvement of the 'vesicular route' in lymph formation. Analogously the numerical increase of the 'intraendothelial channels' in the same period, which was apparent, though we did not perform a statistical analysis, could suggest an active participation of these structures also in the mechanisms of transendothelial transport.

Acknowledgment. This work was supported by a grant from the Ministero Pubblica Istruzione (40%), Rome, Italy.

1 Rhodin, J. A. G., in: Progress in Pyelonephritis, p. 391. Ed. E. H. Kass, F. A. Davis Co, Philadelphia 1965.
2 Bell, R. D., Keyl, M. J., Shrader, F. R., Jones, E. W., and Henry, L. P., Nephron *5* (1968) 454.
3 Dieterich, H. J., and Kriz, W., Pyelonephritis *3* (1972) 1.
4 Albertine, K. H., and O'Morchoe, C. C. C., Lymphology *13* (1980) 100.
5 Niiro, G. K., and Jarosz, H. M., O'Morchoe, P. J., and O'Morchoe, C. C. C., Am. J. Anat. *177* (1986) 21.
6 Vogel, G., Gärtner, K., and Ulbrich, M., Lymphology *7* (1974) 136.
7 O'Morchoe, C. C. C., in: Experimental Biology of the Lymphatic Circulation, vol. 9, p. 261. Ed. M. G. Johnston. Elsevier Science Publishers, Amsterdam 1985.
8 Peirce, E. C., Anat. Rec. *90* (1944) 315.
9 Nordquist, R. E., Bell, R. D., Sinclair, R. J., and Keyl, M. J., Lymphology *6* (1973) 13.
10 Rojo-Ortega, J. M., Yeghiayan, E., and Genest, J., Lab. Invest. *29* (1973) 336.
11 Eliska, O., Lymphology *17* (1984) 135.
12 Holmes, M. J., O'Morchoe, P. J., and O'Morchoe, C. C. C., Am. J. Anat. *149* (1977) 333.
13 Cuttino, J. T., Jennette, J. C., Clarck, R. L., and Kwock, L., Lymphology *18* (1985) 24.
14 O'Morchoe, C. C. C., Lymphology *18* (1985) 2.
15 O'Morchoe, C. C. C., O'Morchoe, P. J., Holmes, M. J., and Jarosz, H. M., Lymphology *11* (1978) 27.
16 Ottaviani, G., and Giacomelli, V., Ateneo Parmense *26*, Suppl. *3* (1955) 3.
17 Reynolds, E. S., J. Cell Biol. *17* (1963) 208.
18 Jones, W. R., O'Morchoe, P. J., and O'Morchoe, C. C. C., Microvasc. Res. *25* (1983) 286.
19 Werner, G., Meth. - Elmi *7* (1975) 4.

20 Comparini, L., and Bastianini, A., Arch. it. Anat. Embriol. *72* (1967) 59.
21 Ohkuma, M., Lymphology *6* (1973) 175.
22 McIntosh, G. H., and Morris, B., J. Physiol., Lond. *214* (1971) 365.
23 Cockett, A. T. K., Roberts, A. P., and Moore, R. S., Invest. Urol. *7* (1970) 266.
24 O'Morchoe, P. J., Yang, V. V., and O'Morchoe, C. C. C., Microvasc. Res. *20* (1980) 275.
25 O'Morchoe, C. C. C., Jarosz, H. M., Jones, W. R., and O'Morchoe, P. J., in: Endothelial Cell Vesicles; Prog. appl. Microcirc., vol. 9, p. 88. Karger, Basel 1985.
26 Azzali, G., Arch. it. Anat. Embriol. *85* (1980) 391.
27 Azzali, G., J. submicrosc. Cytol. *14* (1982) 45.
28 Azzali, G., Lymphology *15* (1982) 106.
29 Wailand, H., and Silberberg, A., Microvasc. Res. *15* (1978) 367.
30 Kayser, C., Ann. Biol. *29* (1953) 109.

0014-4754/88/050441-04$1.50 + 0.20/0

Distal axonopathy in streptozotocin diabetes in rats

S. Chokroverty*, D. Seiden, P. Navidad and R. Cody

The Neurology Service, VA Medical Center, Lyons (New Jersey 07939, USA), and the Departments of Neurology, Anatomy and Environmental and Community Medicine, UMDNJ-Robert Wood Johnson Medical School, New Brunswick and Piscataway (New Jersey, USA)
Received 11 January 1988; accepted 23 February 1988

Summary. We noted the earliest morphological changes in the motor endplates 8 weeks after the induction of streptozotocin diabetes in rats. Morphometric measurements showed reduced axonal areas of the lateral plantar and the sciatic nerves in the diabetic rats 28 but not 2 and 8 weeks after the experiment. These findings suggested distal axonopathy.
Key words. Streptozotocin; rats; diabetic; distal; axonopathy.

The pathogenesis of diabetic neuropathies remains elusive[1,2] and the search for underlying mechanisms is hampered by the lack of a satisfactory animal model. Nerve conduction studies have shown reduced conduction velocities early in the course of experimental diabetes[3–5], however, morphological correlates have not been consistently identified. Several morphological abnormalities in the somatic nerves have been reported: axonal degeneration and atrophy[6], endoneurial edema[6], distal axonopathy[7,8], demyelinating neuropathy and axonal degeneration[9], axonal shrinkage[10] due to hyperosmolar state rather than axonal atrophy and a lack of structural alterations, and minor changes related to growth inhibition and maturational deficits in diabetic animals[11]. We wish here to report morphological changes in the distalmost part of the lower motor neuron of streptozotocin-induced diabetic rats proceeding proximally in the course of time.

Methods. Charles River Strain (Charles River Breeding Company, Wilmington, Mass.) of Sprague-Dawley adult male rats weighing 180–200 g were injected with streptozotocin (50 mg/kg b. wt) into the tail vein to induce experimental diabetes mellitus. All rats were housed in cages under identical circumstances and given free access to water and Purina Rat Chow. We followed the Institution's guide for the care and use of laboratory animals. Age and weight matched male rats were used for controls receiving no injections. There were 5–9 rats in each group (diabetic vs control).

Before sacrifice at the end of 2, 8 and 28 weeks, blood was collected from the tail vein of each animal for glucose assay. The animals were then weighed and lightly anesthetized with nembutal. Perfusion-fixation of the hind limbs was accomplished at room temperature through the abdominal aorta with 2.5% glutaraldehyde in 0.2 N cacodylate buffer at a pH of 7.2. A strip of muscle was removed from the medial gastrocnemius muscle in the region of the motor points and fixed in 2.5% glutaraldehyde for studying motor endplate fine structure. Portions of the sciatic nerve from the proximal and distal segments, the tibial nerve close to its insertion into the medial gastrocnemius muscle and the lateral plantar nerve were removed and fixed in glutaraldehyde.

We used a modification[12] of Engel's technique for localizing the endplate for electron microscopy. A Zeiss MOP-3 manual optical picture analyzer was used to measure the presynaptic and postsynaptic membrane length, the nerve terminal and postsynaptic areas of the motor endplate fine structure. The nerve specimens were embedded in an epon-araldite mixture, and semithin sections (1–1.5 μm in thickness) in cross sections were stained with toluidine blue and photographed at a final magnification of 1000 x for measurement of the axonal areas. Ultrathin sections of the nerves were then cut on an ultramicrotome and examined by electron microscopy.

Morphological data were subjected to qualitative and quantitative analysis using a 2-tailed Student's t-test. The dependent variables were also analyzed using analysis of variance (ANOVA).

Results. Rats injected with streptozotocin remained diabetic as evidenced by hyperglycemia and glucosuria throughout the experiment. They lost weight considerably in the first 2 weeks, but then showed a slight weight gain which was much less than the weight gained by the control rats (table 1). A two-way (group × time) ANOVA was performed with time as a repeated measure on the variables, weight change and blood glucose (table 1). No significant relationship was found between the blood glucose and weight loss between the diabetic and control animals. The diabetic rats developed cataracts after 8 weeks.

Morphological observations. There was no significant difference between the values in different segments of the sciatic-tibial-lateral plantar nerves in the control and diabetic rats at

Table 1. Mean weight (g) change (gain +; loss −) and mean blood glucose (mg/dl) in diabetic and control rats

Group	Determination	2 weeks	8 weeks	28 weeks
Control rats	Blood glucose	89.0	86.3	91.1
	Weight change	+ 72.0	+ 181.3	+ 335.6
Diabetic rats	Blood glucose	320.3	338.7	424.2
	Weight change	− 72.7	+ 1.9	+ 22.2